Performance-Optimized Quantization for InSAR Applications

Michele Martone[a], Nicola Gollin[a], Paola Rizzoli[a], and Gerhard Krieger[a]
[a]Microwaves and Radar Institute, German Aerospace Center, 82234 Wessling, Germany

Abstract

For present and next-generation spaceborne SAR missions, an increasing volume of onboard data is going to be demanded, which implies, from the mission design point of view, more stringent requirements in terms of onboard memory and downlink capacity. In this scenario, an efficient quantization of the SAR raw data is of primary importance, since the data rate employed for raw data digitization defines the amount of data to be stored and transmitted to the ground and directly affects the performance of the resulting SAR products. In this paper, a novel performance-optimized block-adaptive quantization (PO-BAQ) is introduced. PO-BAQ exploits state-of-the-art quantization algorithms for SAR systems, and aims at optimizing the resource allocation and, at the same time, the interferometric performance in the resulting InSAR products, by exploiting a priori knowledge of the local SAR backscatter statistics. Analyses on experimental TanDEM-X interferometric data are presented. The obtained results can be combined with the precise, high-resolution knowledge of the Earth's topography and backscatter characteristics, in order to provide a helpful tool for performance budget definition and optimization of the resource allocation strategies for future SAR missions.

1 Introduction

Synthetic aperture radar (SAR) represents nowadays a well-recognized technique for a large variety of remote sensing applications, being able to acquire high-resolution images of the Earth's surface, independently of daylight and weather conditions. Interferometric SAR (InSAR) exploits the *phase difference* of at least two complex SAR images, acquired from different orbit positions and/or at different times. The derived information allows for the estimation and assessment of many geophysical parameters, such as ocean currents, ground deformations, and Earth's topography, through the generation of digital elevation models (DEMs). In the last decades, innovative spaceborne radar techniques have been proposed to overcome the limitations imposed by "conventional" SAR imaging for the acquisition of wider swaths and, at the same time, of finer azimuth resolutions. Clearly, this is associated with the demand of gathering an increasing amount of information in a shorter time interval, which implies harder requirements in terms of on-board memory and downlink capacity. This aspect represents a critical issue for all spaceborne SAR missions and, in turn, directly dictates a trade-off between the quality of the resulting SAR products and the sensor acquisition capabilities. Such systems are often designed so that a certain degree of correlation and redundancy is present in the SAR raw data, hence opening up new opportunities for efficient onboard data volume reduction, as presented in the context of, e.g., multi-channel SAR and staggered SAR systems [1], [2], [3]. In this scenario, the proper digitization of the SAR raw data represents an aspect of utmost importance, as the quantization rate defines the amount of data to be stored and transmitted to the ground and it directly affects the performance of the SAR products. This paper investigates quantization effects on TanDEM-X InSAR data. TanDEM-X (TerraSAR-X add-on for Digital Elevation Measurement) is the first bistatic SAR mission able to perform single-pass interferometric acquisitions with the opportunity of variable baseline selection [4]. While being a very flexible and powerful system, the acquisition capabilities of the TerraSAR-X and TanDEM-X satellites are constrained by their relatively short orbit duty cycle (about 3 minutes per orbit) and limited onboard memory (of 256 Gbit and 512 Gbit, respectively), which pose constraints on the achievable data rate during the mission: indeed, about one year was required to complete one global acquisition of the Earth's landmasses fulfilling the mission specifications [4].
Starting from the present considerations, we introduce a novel performance-optimized block-adaptive quantization (PO-BAQ) method, which extends the concept of the state-of-the-art BAQ and aims at optimizing the resource allocation together with the resulting interferometric performance. In particular, the interferometric phase error is chosen as metric for performance optimization, but the proposed method can in principle be extended by using any performance measure required for the specific SAR applications, such as the image signal-to-noise ratio (SNR), the height accuracy of the resulting DEM, or the accuracy of the information derived from higher-level products (like, e.g., terrain deformation or the accuracy of specific classification methods).
The paper is organized as follows. Section 2 presents the impact of raw data quantization on SAR imaging and interferometric performance of bistatic TanDEM-X data. The performance-optimized block-adaptive quantization (PO-BAQ) is described in Section 3 and preliminary examples are shown, which demonstrate the effectiveness of the proposed method. Section 4 concludes the paper with an outlook on future research.

Table 1 σ_{σ^0} and BAQ rates required for achieving a phase error of 5° and 10° for the test acquisitions shown in Figure 1.

Test Site	σ_{σ^0}	$N_{b,req}$ for $\sigma_{\Delta\varphi_{req}} = 5^\circ$	$N_{b,req}$ for $\sigma_{\Delta\varphi_{req}} = 10^\circ$
Greenland - snow & ice, flat	5.8 dB	2.5 bps	<2 bps
Iowa (USA) - agricultural, flat	6.1 dB	3.5 bps	2.1 bps
Rondônia (Brazil) - rainforest, flat	6.6 dB	3.6 bps	2.5 bps
Death Valley (USA) - soil & rock, mountainous	7.0 dB	4.4 bps	2.8 bps
Las Vegas - urban, flat	7.4 dB	5.1 bps	3.5 bps
Mexico City - urban, mountainous	8.1 dB	5.6 bps	3.8 bps
Malaysia - tropical forest, mountainous	8.2 dB	5.9 bps	4.8 bps

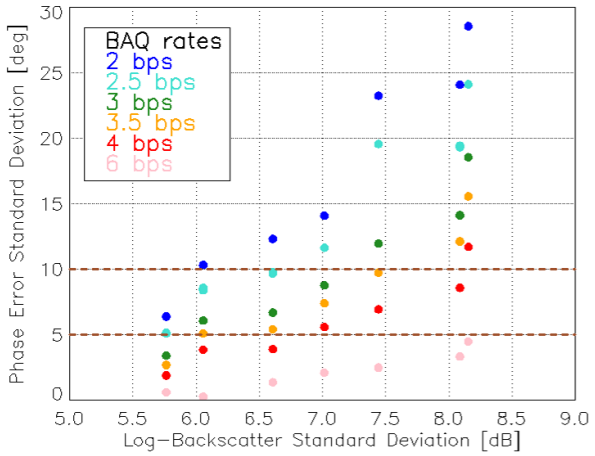

Figure 1 Standard deviation of the phase error due to quantization $\sigma_{\Delta\varphi}$ as a function of the standard deviation of the radar backscatter σ_{σ^0} for different BAQ rate configurations. Each value of σ_{σ^0} corresponds to a different test site, listed in Table 1. The two horizontal brown lines trace exemplary phase error requirements of 5° and 10°, from which the minimum BAQ rate can be derived, as summarized in Table 1.

2 Quantization Effects in TanDEM-X InSAR Data

In this section the impact of SAR raw data quantization on the interferometric phase errors is investigated, with particular focus on those system and scene parameters which most affect SAR quantization errors. Together with the BAQ compression rate N_b, the degree of inhomogeneities in the backscatter distribution, quantified by the standard deviation of the SAR backscatter σ_{σ^0} have been evaluated over selected test areas showing different land cover types and topographic characteristics, which are summarized in Table 1. The experimental TanDEM-X data takes, acquired with full analog-to-digital converter (ADC) resolution of 8 bits/sample (bps), have been re-compressed on ground using BAQ at 2, 3, 4, and 6 bps. Then, SAR images and interferograms have been generated by using the experimental TanDEM-X interferometric processor (TAXI), developed at DLR [5]. The combination of different compression rates for the master and the slave acquisition allows for the implementation of non-integer BAQ rates (e.g., 3-bit BAQ for the master and 2-bit BAQ for the slave leads to an equivalent 2.5-bit for the resulting interferometric products) [6], [7]. Figure 1 shows the standard deviation of the interferometric phase error $\sigma_{\Delta\varphi}$ as a function of the standard deviation of the SAR backscatter σ_{σ^0} for different quantization rates. The phase error is calculated as the difference between the interferometric phase obtained from raw data quantized at different BAQ rates, and the uncompressed one (BAQ-bypass, 8-bit ADC). Each dot represents the value obtained from a single SAR acquisition and bit rate. The test areas are summarized in Table 1 and have a typical extension of 30 km in ground range and between 25 km and 50 km in azimuth. In this analysis, the InSAR data have been processed to an interferometric posting $\Delta p = 12$ m, which, given the typical azimuth and range resolution of TanDEM-X, results in number of looks N_l ranging between 14 and 30. From the figure, it can be noticed that σ_{σ^0} and $\sigma_{\Delta\varphi}$ are positively correlated and, as expected, larger phase errors are obtained for heterogeneous regions, such as urban areas or mountainous terrain. The two horizontal brown lines trace exemplary phase error requirements of 5° and 10°, from which the minimum required BAQ rate is provided in Table 1. The specific values reported in the table have been obtained by reprocessing the uncompressed raw data to several fractional quantization rates, which can be implemented by toggling the integer BAQ rate along azimuth (and/or range) as described in [6]. As an example, Figure 2 shows the radar backscatter σ^0 for the test site over (a) the agricultural area in Iowa (USA) and (b) the urban area of Mexico City. The former (Figure 2(a)) shows flat terrain and a rather homogeneous backscatter distribution ($\sigma_{\sigma^0} \approx 6$ dB), resulting in a phase error up to about 10° obtained for the 2-bit BAQ case (Figure 1); the latter (Figure 2(b)) is characterized by heterogeneous backscatter due to the presence of urban settlements as well as of rugged terrain (and $\sigma_{\sigma^0} \approx 8$ dB), for which a phase error up to 25° is observed in Figure 1. For this SAR scene, 3.8 bps would be necessary in order to achieve the exemplary phase error requirement of 10°, i.e. almost twice the data rate needed to fulfill the same requirement over the homogeneous test area in Figure 2(a). These effects are consequence of the so-called low-scatterer suppression, described in detail in [7], [8]. Low-scatterer suppression represents a nonlinear and signal-dependent quantization error source (different from granular and clipping noise, since it is visible only after SAR focusing), and significantly impairs the resulting SAR performance.

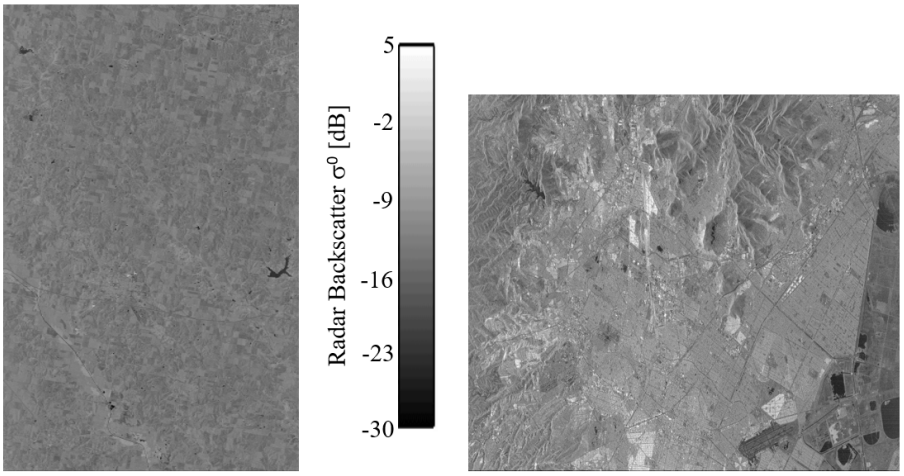

Figure 2 (a) Radar backscatter σ^0 for the test sites over the agricultural area in Iowa (USA). The area extends by about 50 km in azimuth $\times$ 30 km in ground range and shows a standard deviation of the log-backscatter distribution σ_{σ^0} of about 6 dB. (b) σ^0 map for the urban area of Mexico City, extending by 20 km in azimuth $\times$ 35 km in ground range and σ_{σ^0} is of about 8 dB. The impact of quantization errors is larger for scenes showing heterogeneous backscatter distribution, as shown in Figure 1 and Table 1.

In addition to the described parameters, the number of interferometric looks N_l also impacts the resulting phase error. This is, however, a well-known effect (with $\sigma_{\Delta\varphi} \propto \frac{1}{\sqrt{N_\mathrm{l}}}$) and therefore not further investigated in this paper.

Once the relation between quantization errors and backscatter distribution has been verified for the considered SAR acquisitions, the goal is now to investigate the opportunity to refine the performance optimization and bit rate allocation at sub-scene level. Indeed, in a SAR acquisition the responses of the scatterers under illumination overlap in the raw data domain within an area

$$A_\mathrm{SAR} = L_\mathrm{chirp} \times L_\mathrm{s}. \tag{1}$$

L_chirp is the chirp length and L_s is the synthetic aperture which, in turn, are defined as

$$L_\mathrm{chirp} = \frac{c\tau_p}{2}, \quad L_\mathrm{s} = \lambda \frac{R_0}{L_a}, \tag{2}$$

where c is the light velocity, τ_p indicates the chirp pulse duration, R_0 is the slant range, and L_a represents the azimuth antenna length. According to that, each SAR image and interferogram is divided into blocks of size A_SAR, the local statistics and the resulting performance are then evaluated for each block. The results are shown in Figure 3 for the test area of Death Valley (USA) and different quantization rates, and a strong correlation between backscatter heterogeneity and phase error can be once again verified. For completeness, the radar backscatter map σ^0 of the considered area is provided in Figure 5(a).

3 Performance-Optimized Block-Adaptive Quantization (PO-BAQ)

The results shown in the previous section are exploited to optimize the resource allocation (i.e., the commanded BAQ rate) by controlling, at the same time, the resulting phase error degradation. According to the proposed performance-optimized block-adaptive quantization (PO-BAQ), the bit rate $N_\mathrm{b,req}$ to be employed for SAR raw data compression is determined as a function of the considered parameters as

$$N_\mathrm{b,req} = f\left(N_\mathrm{l}, N_\mathrm{acq}, \Delta\varphi_\mathrm{req}, \sigma_{\sigma^0}\right). \tag{3}$$

In the above equation, the number of looks N_l is defined by the system resolution and the target posting, the number of available acquisitions N_acq is typically defined at mission planning (in general, N_acq can be interpreted as a sort of "temporal" looks, hence contributing to mitigate the resulting phase error in the same way as N_l); σ_{σ^0} is estimated from the local backscatter information, and has therefore to be available as external input before data take commanding; $\Delta\varphi_\mathrm{req}$ indicates the maximum allowed phase error due to quantization, and has to be given as input as well. Finally, the function $f(\cdot)$ in (3) is described by the information shown, as an example, in Figure 3, which can be regarded as a sort of look-up-table (LUT) providing a statistical characterization of the performance degradation using real data as input source.

According to the proposed PO-BAQ, the procedure to derive the bit rate to quantize the raw data associated to a given SAR image block is described as follows:

Step 1: Once $\Delta\varphi_\mathrm{req}$, N_l, and N_acq are fixed, the standard deviation of the SAR backscatter block σ_{σ^0} is calculated. In the following, without loss of generality $N_\mathrm{acq} = 1$ is assumed and the performance requirement is expressed in terms of the standard deviation of the phase error, i.e., $\Delta\varphi_\mathrm{req} = \sigma_{\Delta\varphi,\mathrm{req}}$, as depicted in Figure 1 and Figure 3.

Step 2: The phase error values $\sigma_{\Delta\varphi}$ associated with the estimated σ_{σ^0} are fetched from the available information (as

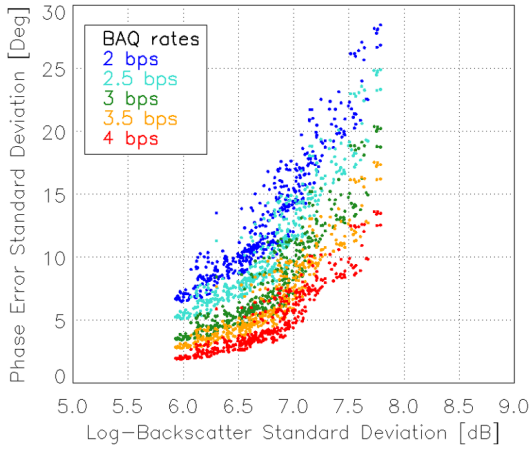

Figure 3 Phase error standard deviation due to quantization $\sigma_{\Delta\varphi}$ as a function of the standard deviation of the backscatter coefficient σ_{σ^0} calculated for image blocks of area A_{SAR} of the test area located in the Death Valley (USA) for different BAQ configurations.

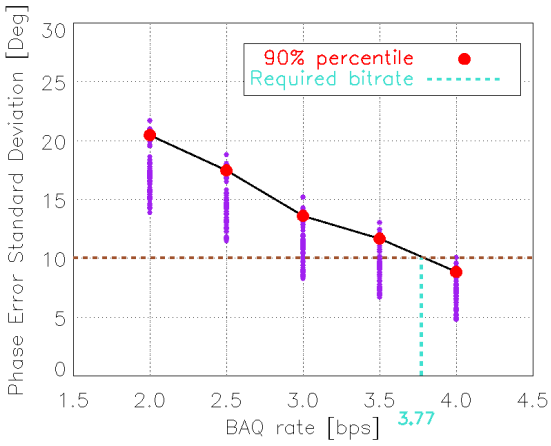

Figure 4 Estimation of the required number of bits ($N_{\mathrm{b,req}} = 3.77$ bps) according to the proposed PO-BAQ for a SAR backscatter block with σ_{σ^0} between 7 dB and 7.25 dB for $N_{\mathrm{l}} = 16$ looks, $\sigma_{\Delta\varphi,\mathrm{req}} = 10^{\circ}$.

shown in Figure 3), which is determined by the actual number of looks N_{l} and for the available bit rate combinations. For this, the range of values of σ_{σ^0} in the look-up table in Figure 3 is subdivided in intervals: Figure 4 shows, as an example, the phase error values (in purple) as a function of the bit rate N_{b} obtained for the image blocks of the test area in Death Valley depicted in Figure 3 for σ_{σ^0} between 7 dB and 7.25 dB (and $N_{\mathrm{l}} = 16$ looks).

Step 3: For each N_{b}, the representative phase error $\sigma_{\Delta\varphi}$ is calculated as the 90$^{\mathrm{th}}$ percentile (big red dots in Figure 4) of the corresponding values distribution (purple dots). Alternatively, another estimator such as, e.g., the maximum value could be chosen: this, however, may result in significantly larger phase error estimates (and, in turn, of the resulting bit rate values $N_{\mathrm{b,req}}$) in case of presence of outliers in the corresponding σ_{σ^0} estimation interval. The resulting values are then linearly interpolated, as indicated by the black line in Figure 4.

Step 4: The number of bits $N_{\mathrm{b,req}}$ required for quantizing the considered SAR raw data block is finally derived as

$$N_{\mathrm{b,req}} = \underset{N_{\mathrm{b}} \in [N_{\mathrm{b,min}}, N_{\mathrm{b,max}}]}{\arg\max} \left\{ \Delta\varphi\left(N_{\mathrm{l}}, \sigma_{\sigma^0}\right) \right\} \quad \text{for} \quad \Delta\varphi \leq \Delta\varphi_{\mathrm{req}}, \tag{4}$$

being $N_{\mathrm{b,min}}$ and $N_{\mathrm{b,max}}$ the minimum and maximum allowed bit rates, respectively, which are typically determined at system/instrument design. As an example, in Figure 4 the dashed horizontal brown line represents $\Delta\varphi_{\mathrm{req}} = \sigma_{\Delta\varphi,\mathrm{req}} = 10^{\circ}$, $N_{\mathrm{b,min}} = 2$ bps, $N_{\mathrm{b,max}} = 4$ bps, and $N_{\mathrm{b,req}} = 3.77$ bps is finally determined as the abscissa corresponding to the intercept between the black line (expected degradation) and the brown one (maximum allowed degradation), and is depicted in turquoise.

Step 5: PO-BAQ can be applied at data take level (i.e., one single $N_{\mathrm{b,req}}$ is derived for the entire SAR acquisition); however, to better exploit the potentials of the proposed method, **Step 1** to **4** are repeated for each block of area A_{SAR} contained in the acquired SAR image, as it has been explained in Section 3. For this purpose, a certain step length d_{step} used for sliding the SAR image block at each iteration, has to be defined. Once all iterations are completed, the output of the PO-BAQ is represented by a two dimensional *bit rate map* (BRM), which contains the quantization rates to be used for that specific SAR acquisition. As it is shown in the example of Figure 4, the resulting rates are typically non-integer numbers, which can be effectively implemented by including additional hardware (e.g., a Huffman coder) [9], or by toggling the integer BAQ rates along azimuth and/or range according to predefined bit rate sequences [6].

Following the example shown in the previous sections, Figure 5(a) depicts the SAR backscatter map σ^0 acquired by TanDEM-X over the Death Valley (USA). The region extends by about 35 km in both, azimuth and range, and is characterized by the presence of non-vegetated, rocky mountains and a rather large dynamic range in σ^0 (see Table 1). Figure 5(b) shows the resulting bit rate map generated according to the proposed PO-BAQ for $N_{\mathrm{l}} = 16$ looks, $N_{\mathrm{acq}} = 1$, and $\sigma_{\Delta\varphi,\mathrm{req}} = 10^{\circ}$. For this example, a step length $d_{\mathrm{step}} = 500$ m in azimuth and range was set, which corresponds to the pixel size of the BRM. As expected, larger values of $N_{\mathrm{b,req}}$, up to 5 bps, are obtained in correspondence of the pronounced topography (lower right part of Figure 5(a)), with respect to the more homogeneous region in the upper half of the image, for which smaller BAQ rates, down to 2 bps, are sufficient to fulfill the phase error requirement. In particular, since the responses of the scatterers under illumination overlap in the raw data domain within an area A_{SAR} (defined in (1)), using a bit rate N_{b} to quantize a portion of raw data affects the final performance, in the focused image, also in areas located in its close vicinity (for TanDEM-X, the synthetic aperture L_{s} and the chirp length L_{chirp} are in the order of a few kilome-

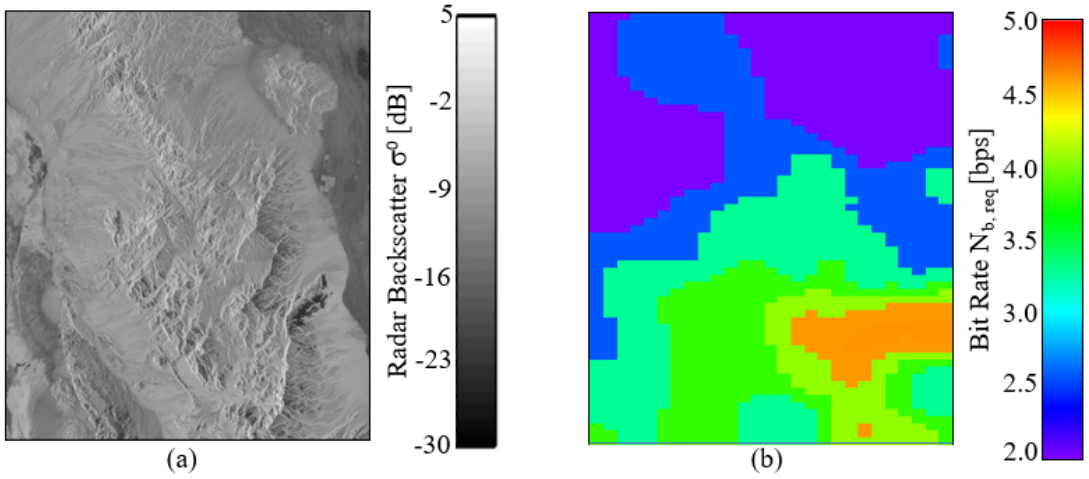

Figure 5 (a) Radar backscatter σ^0 of the test area located in the Death Valley (USA), which extends over about 35 km both in azimuth (vertical) and range (horizontal dimension). (b) Bit rate map (BRM) generated according to the proposed PO-BAQ ($N_{\mathrm{b,req}}$ in (4)) for $N_{\mathrm{l}} = 16$ looks, $N_{\mathrm{acq}} = 1$, and $\sigma_{\Delta\varphi,\mathrm{req}} = 10^{\circ}$. The average bit rate $\overline{N}_{\mathrm{b,req}} = 2.99$ bps.

ters). The described mixing effect of the target responses leads to a low-pass effect in the resulting bit rate map, for which smooth transitions between values of N_{b} are typically observed. Figure 6(a) depicts the phase error map resulting from the BRM in Figure 5(b). Each pixel represents the standard deviation of the phase error due to quantization $\sigma_{\Delta\varphi}$ calculated in the data block, centered in the corresponding pixel, of area A_{SAR}. About 8% of the pixels do not fulfill the requirement of $\sigma_{\Delta\varphi,\mathrm{req}} = 10^{\circ}$, which are highlighted in dark red in the mask in Figure 6(b). This can be explained with the fact that the 90$^{\mathrm{th}}$ percentile of the phase error distributions has been used, for each N_{b} and σ_{σ^0} interval, to derive the resulting $N_{\mathrm{b,req}}$ (as described in **Step 3** and shown in Figure 4). The average bit rate obtained from the BRM in Figure 5(b) is $\overline{N}_{\mathrm{b,req}} = 2.99$ bps. On the other hand, we reported in Table 1 that $N_{\mathrm{b,req}} = 2.8$ bps is needed to achieve a phase error standard deviation of 10°, estimated over the entire scene. With the PO-BAQ, however, we do aim at fulfilling the same requirement, but for each of the image blocks of size A_{SAR}, which justifies the slightly larger (about 7%) average bit rate required. Given that $\overline{N}_{\mathrm{b,req}} = 2.99$ bps it is reasonable to compare the performance of the proposed PO-BAQ with a nominal 3-bit BAQ: Figure 6(c) shows the phase error distribution as function of the standard deviation of the backscatter σ_{σ^0}, calculated in the corresponding SAR intensity image block. With respect to the 3-bit BAQ case (green dots), the distribution of the PO-BAQ values (in purple) appears to be "tilted" horizontally and concentrated below the dashed brown line, which identifies the 10° requirement set as input. Figure 6(d) depicts the histograms of the phase error values for the 3-bit BAQ (green bars) and PO-BAQ (purple bars). Again, the distribution resulting from the 3-bit BAQ shows a large dispersion mostly between 3° and 15°. On the other hand, the values obtained from the PO-BAQ are mostly concentrated between 5° and 10° (depicted in turquoise and yellow in Figure 6(b)), hence demonstrating the effectiveness of the proposed method.

As a comparison with the proposed PO-BAQ, it is worth at this point to recall the principle of the flexible dynamic block-adaptive quantization (FDBAQ) [9] for onboard data compression on the C-band Sentinel-1 SAR satellites. The FDBAQ extends the concept of block-adaptive quantization (BAQ), by adaptively adjusting the quantization rate according to the local SNR [9]. Such an optimization of performance and data rate is achieved in the raw data domain, and therefore the actual degradation in the focused SAR and InSAR products is not taken into account, which indeed represents the main advantage of the method introduced in this paper. In addition, FDBAQ exploits average backscatter statistics at C band to associate the desired bit rate to each σ^0 range. On the other hand, the implementation of the PO-BAQ relies on the a priori knowledge of accurate SAR backscatter information, down to a few kilometers scale, for the derivation of the BRM. Since the bit rate is determined before the data take commanding, the total required volume of data is known in advance, but the bit rate information needs to be uplinked and implemented on the sensor, which may require additional on-board computational and processing effort (differently from the FDBAQ, where the data rate is estimated on board from the statistics of the received raw data samples [9]).

4 Conclusions and Outlook

Quantization errors in SAR data are significantly influenced by the local backscatter statistics in the SAR image. In this paper, we introduced a novel performance-optimized BAQ which defines the bit rate allocation to a predefined expected performance degradation, and can therefore be adapted to the specific SAR application and requirements. The impact of quantization on the interferometric phase errors of TanDEM-X data has been evaluated and the steps of the PO-BAQ algorithm have been described in detail. The proposed approach has been demon-

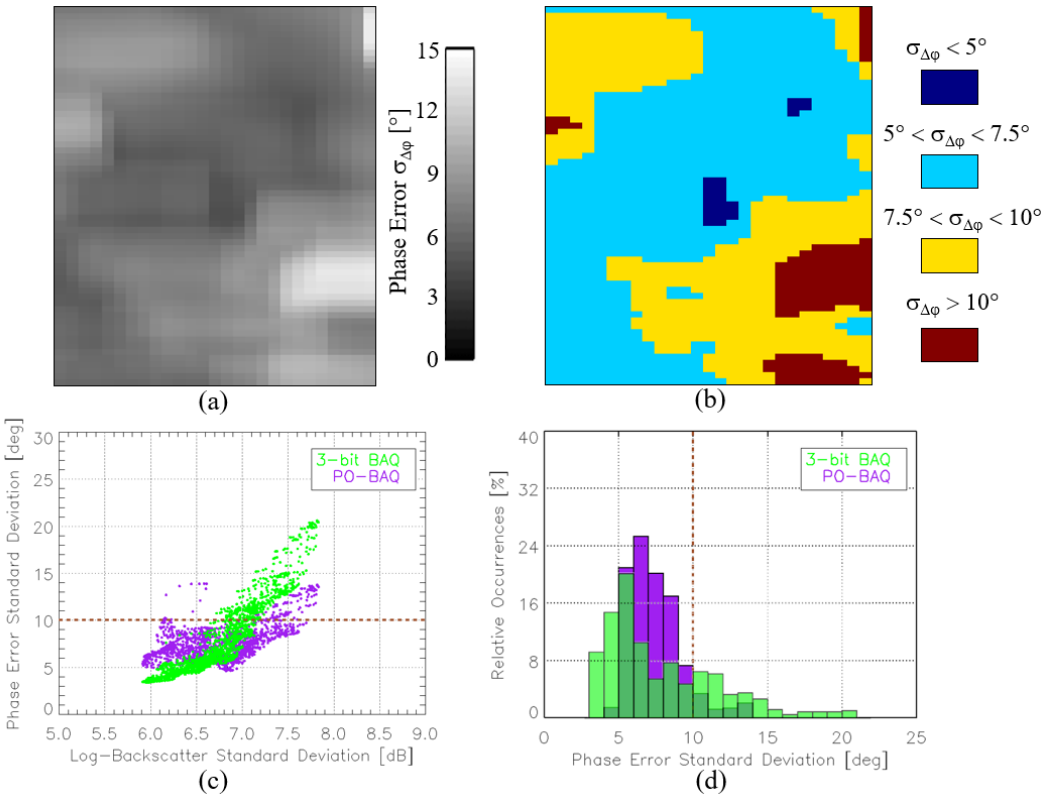

Figure 6 (a) Phase error map resulting from the BRM in Figure 5(b). Each pixel represents the standard deviation of the phase error $\sigma_{\Delta\varphi}$ calculated in the data block of area A_{SAR}. The pixels which do not fulfill the phase error requirement $\sigma_{\Delta\varphi,\mathrm{req}} = 10^{\circ}$ (about 8% of the total) are highlighted in dark red in the mask in (b). (c) Phase error values (taken from the map in (a)) as a function of the standard deviation of backscatter. (d) Corresponding phase error histograms overlaid. The distribution resulting from the 3-bit BAQ (in green) shows a larger dispersion, while the values obtained from the PO-BAQ (in purple) are mostly concentrated between 5° and 10° (depicted in turquoise and yellow in (b)).

strated on real data, and we could verify that the resulting degradation is consistent with the expectation. The present PO-BAQ does not rely on any specific property of the SAR raw signal and can be applied in combination with methods for data volume reduction such as those proposed in [1], [2], or [3].

As a next step, the proposed method will be tested over a larger set of SAR acquisitions, with the goal of better characterizing the performance for different land cover characteristics, in order to ultimately provide a helpful tool for performance and data rate optimization for present and future SAR missions.

5 Literature

[1] M. Martone et al.: Efficient onboard quantization for multi-channel SAR systems, IEEE Geosci. and Remote Sens. Lett., 2019.

[2] P. Guccione et al.: Principal components dynamic block quantization for multi-channel SAR, IEEE Int. Geosci. Remote Sens. Symp., pp. 1034-1037, Bejing (China), July 2016.

[3] M. Martone et al.: Predictive quantization for data volume reduction in staggered SAR systems, IEEE Trans. Geosci. and Remote Sens. Vol. 58, No. 8, pp. 5575-5587, Aug. 2020.

[4] G. Krieger et al.: TanDEM-X: A satellite formation for high-resolution SAR interferometry, IEEE Trans. Geosci. and Remote Sens. Vol. 45, No. 11, pp. 3317-3341, Nov. 2007.

[5] P. Prats et al.: TAXI: A versatile processing chain for experimental TanDEM-X, Proc. Int. Geosci. Remote Sens. Symp., 4059-4062, Honolulu, Hawaii (USA), Jul. 2010.

[6] M. Martone et al.: Azimuth switched quantization for SAR systems and performance analysis on TanDEM-X data, IEEE Geosci. and Remote Sens. Lett., Vol. 11, no. 1, pp. 181-185, Jan. 2014.

[7] M. Martone et al.: Quantization effects in TanDEM-X data, IEEE Trans. Geosci. and Remote Sens., Vol. 53, no. 2, pp. 583-597, Feb. 2015.

[8] S. Huber et al.: The TanDEM-X mission: Overview and interferometric performance, Int. J. Microw. Wireless Technol., Vol. 2, no. 3-4, pp. 379-389, Jul. 2010.

[9] E. Attema et al.: Flexible dynamic block adaptive quantization for Sentinel-1 SAR Missions, IEEE Geosci. and Remote Sens. Lett., Vol. 7, no. 4, pp. 766-770, Oct. 2010.